Design and Analysis of the Load Adaptive IPT System Applied to Underwater Docking System

Mingwei Lin, Canjun Yang, Dejun Li, Tao Zhang, Tianlei Wang
The State Key Laboratory of Fluid Power and Mechatronic Systems
Zhejiang University, Zheda Road 38, Hangzhou, 310027, China

***Abstract*-Inductive power transfer (IPT) is widely used for the contactless charging system. In an underwater environment, it's also a feasible way to the underwater vehicles for battery charging. In this paper, a novel design process of IPT system is implemented. Serial-serial (SS) topology is selected for the application due to the constant output voltage in a non-resonant state even with a various load. The experiment of the IPT system verifies the theoretical analysis and demonstrates a high efficiency about 80% with a maximum charging power of 300 watts via the water of 1.5 cm's thickness.**

Keywords—Inductive power transfer (IPT), battery charging, docking system, load adaptability

Nomenclature

C_1, C_2 Compensation capacitance of the primary and secondary coil
M Mutual inductance between two coils
L_1, L_2 Inductance of the primary coil and secondary coil
I_{C1}, I_{C2} Primary capacitor current and secondary capacitor current
I_P, I_S Primary winding current and secondary winding current
I_1, I_L Source current and load current
V_1, V_L Source voltage and load voltage
ω Operating angular frequency
R_1, R_2 DC resistance of the self-inductance L_1, L_2
d_1, d_2 Diameter of the primary coil and secondary coil
P_{mchar} Maximum charging power
d Gap between two windings

I. *Introduction*

Autonomous underwater vehicles (AUVs) are widely used for the deep-sea exploration. However, its working duration is always limited by the battery capacity. To enhance the cruising ability of the AUV, it's advisable to build up an underwater docking station for recharging.

Several research institutions have carried out the pool, the lake and the sea trials to test the function and stability of the charging system. There are two common method for AUVs' recharging applied to the docking station, IPT type and plug type. Kojiya et al.(2004) utilized a pair of cone-type coil to realize inductive power transfer about 500 watts at about 96% efficiency when the diameter of coil is 48mm.The dock designed by Robert et al.(2008) was a fixed-heading cone without the requirement for the vehicle to carry an external latching mechanism. The efficiency of the inductive units was 77% with an overall power system efficiency of 48%. Allen et al. (2006) proposed a plug-type device with two guide pins. The electrical connector is inside the shortest pin in the middle. Pyle et al. (2012) leveraged a large UUV platform with a docking station to enable forward basing and persistence for the light weight AUVs. Inductive power transferred from the UUV to the AUV at 450 watts (15 amps/30 volts) with the design of being capable of 1.5KWh power transfer. In addition, Fukuda et al. (2013) demonstrated a new concept of sharing one pair of antennas for

978-1-5090-1537-5/16/$31.00 ©2016 IEEE

contactless communication and power transmission.

In this paper, a pair of coaxial spiral coils is designed for the docking system. The primary coil is fixed outside the AUV and the secondary coil is mounted in the docking station. Furthermore, SS topology is selected for the application due to the constant output voltage, which is proportional to the input voltage in a non-resonant state. A detailed method is introduced to select the parameters of the

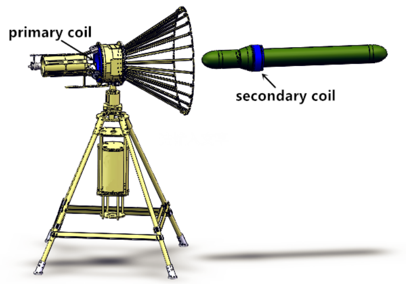

Fig.1 Structural representation of the coils

system. The experimental result shows a higher efficiency during the charging process about 80% and verifies the stability of the charging system via the water of a 1.5 cm's thickness.

II. Structure of coils

A pair of coaxial coreless coils is shown in Fig.1. Litz wire is tightly wound around the nylon bushing and sealed by the epoxy resin glue. The windings are connected to the PCB inside the AUV by the water-proof connectors. The secondary coil is fixed outside the AUV and the primary coil is mounted in the docking station. Fig.2 demonstrates a close-up of the coils. The designed volume of the secondary coil should be limited to avoid higher fluid resistance to the AUV and the primary coil should be larger than the secondary side to ensure the successful docking and the contactless power transfer. Therefore, the parameters of windings are prefixed in the hardware design.

III. Design and analysis of IPT system

A.Characteristics of the circuit

SS topology is a commonly-used loosely

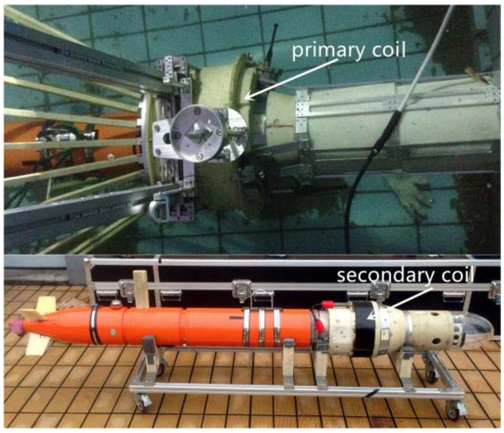

Fig.2 Close-up of two coils

coupled transformer prototype, as shown in Fig.3.Two compensation capacitors C_1 and C_2 are utilized to eliminate the reactive component in the circuit for higher transfer efficiency. However, during the charging process, the equivalent load changes as the charging power varies, which results in the fluctuant output voltage. In general, a voltage regulator is used for the charging system to keep a constant output voltage for normal operating.

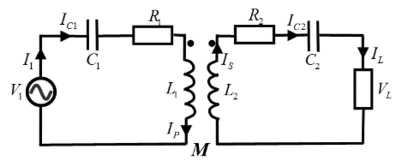

Fig.3 SS compensation

But the fluctuant output voltage may not satisfy the input range of the regulator with the conventional resonant compensation. Thus an original method is proposed to design the circuit with a stable output voltage in a non-resonant state.

In order to analyze the output voltage, the relationship of compensation capacitors, operating frequency, load and output voltage should be derived firstly.

The secondary series impedance is given by

$$Z_2 = j\omega L_2 + \frac{1}{j\omega C_2} + R_L + R_2 \tag{1}$$

Boys et al. (2000) gives the value of resistance reflected to primary circuit in following equation

$$Z_r = \frac{(\omega M)^2}{Z_2} \quad (2)$$

So the source current $\vec{I_1}$ and primary winding current $\vec{I_p}$ are given by

$$\vec{I_1} = \vec{I_P} = \frac{\vec{V_1}}{Z_r + R_1 + j\omega L_1 + \frac{1}{j\omega C_1}} \quad (3)$$

Where $\vec{V_1} = V_1\angle 0°$. V_1 denotes the effective value of $\vec{V_1}$. The denominator of the equation (3) represents the total input impedance $Z_{in} = Z_r + R_1 + j\omega L_1 + \frac{1}{j\omega C_1}$. According to the characteristics of the mutual-inductance circuit, the secondary winding current $\vec{I_S}$ is obtained as

$$\vec{I_S} = \frac{j\omega M \vec{I_P}}{Z_2} \quad (4)$$

Therefore, the load voltage is given by

$$\vec{V_L} = \vec{I_S} R_L = \vec{I_L} R_L = \frac{j\omega M R_L \vec{V_1}}{(j\omega L_2 + \frac{1}{j\omega C_2} + R_L + R_2)(Z_r + R_1 + j\omega L_1 + \frac{1}{j\omega C_1})} \quad (5)$$

$M_V = \frac{|\vec{V_L}|}{|\vec{V_1}|} = \left|\frac{\vec{V_L}}{\vec{V_1}}\right|$ denotes the voltage ratio and assume $R_1 = R_2 = 0$ due to their negligible effect in the circuit.

So

$$M_V = \left| \frac{j\omega M R_L}{(j\omega L_2 + \frac{1}{j\omega C_2} + R_L)(\frac{(\omega M)^2}{j\omega L_2 + \frac{1}{j\omega C_2} + R_L} + j\omega L_1 + \frac{1}{j\omega C_1})} \right| \quad (6)$$

Let $A(\omega) = \omega L_1 - \frac{1}{\omega C_1}$ and $B(\omega) = \omega L_2 - \frac{1}{\omega C_2}$, M_V can be simplified as following

$$M_V = \left| \frac{j\omega M R_L}{[\omega^2 M^2 + jA(\omega)(jB(\omega) + R_L)]} \right| = \left| \frac{j\omega M R_L}{[\omega^2 M^2 - A(\omega)B(\omega)] + jR_L A(\omega)} \right| \quad (7)$$

Let $Q(\omega) = \omega^2 M^2 - A(\omega)B(\omega)$, and $A(\omega)$ and $Q(\omega)$ cannot be both zero. So we have

$$M_V = \left| \frac{j\omega M R_L}{Q(\omega) + jR_L A(\omega)} \right| = \frac{\omega M R_L}{\sqrt{A^2(\omega) R_L{}^2 + Q^2(\omega)}} \quad (8)$$

If the system is in completely resonance, $\omega = \frac{1}{\sqrt{L_1 C_1}} = \frac{1}{\sqrt{L_2 C_2}}$ .So the equation (8) can be simplified as

$$M_V = \frac{R_L}{\omega M} \quad (9)$$

It's obvious that the output voltage is proportional to the load with the completely resonant compensation. So this compensation may be not suitable for the battery charging due to the variational load.

Simplifying the equation (8) above, we have

$$[M_V{}^2 A^2(\omega) - \omega^2 M^2] R_L{}^2 + M_V{}^2 Q^2(\omega) = 0 \quad (10)$$

In order to keep a constant M_V, the output voltage shouldn't change as the load varies.

Therefore, the following condition should always hold

$$M_V{}^2 A^2(\omega) - \omega^2 M^2 = 0$$

$$\Rightarrow M_V = \frac{\omega M}{\omega L_1 - \frac{1}{\omega C_1}} = \frac{\omega^2 M C_1}{\omega^2 L_1 C_1 - 1} \qquad (11)$$

$$Q(\omega) = 0 \Rightarrow \omega^2 M^2 = (\omega L_1 - \frac{1}{\omega C_1})(\omega L_2 - \frac{1}{\omega C_2})$$

$$\Rightarrow \omega^4 C_1 C_2 (M^2 - L_1 L_2) + \omega^2 (L_1 C_1 + L_2 C_2) - 1 = 0 \qquad (12)$$

In equation(11)、(12), the mutual inductance M and self-inductance L_1, L_2 of two windings are known quantity. According to the value of the input voltage, the relationship of the angular frequency ω and compensation capacitors C_1, C_2 are determined.

The efficiency of the IPT system is given by

$$\eta = \frac{P_{out}}{P_{in}} = \frac{I_L V_L}{I_1 V_1} = \frac{(\omega M)^2 \sqrt{Q^2(\omega) + A^2(\omega) R_L^2}}{A^2(\omega) R_L \sqrt{R_L^2 + B^2(\omega)}} \qquad (13)$$

As can be seen from the equation (13), the efficiency of the IPT system is unacted on the input voltage. When the geometrical (a) parameters of two coils are determined with a constant output voltage, the transfer efficiency only depends on the operating frequency and the equivalent load.

B.Analysis and Selection of System Parameters

During the charging process (CC-CV for the lithium battery), the power transferred to the battery pack generally varies between P_{mchar} /10 and P_{mchar} .The conventional resonant compensation may not always ensure an output voltage within the input range of the regulator. In Fig.4, the output voltage is

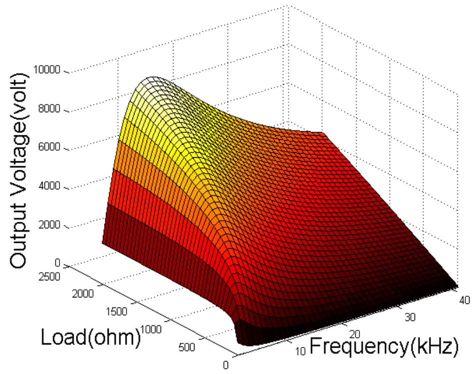

Fig.4 Output voltage versus different frequency at various load model

largely fluctuant as the load varies in the completely resonance for SS topology. To output a stable voltage, the compensation

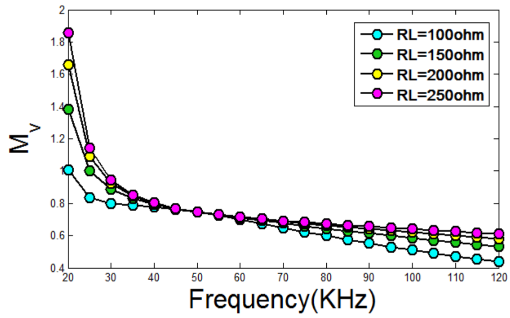

(a)

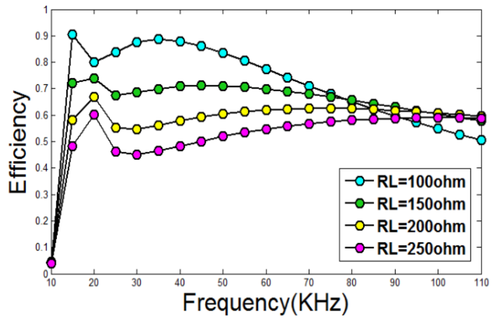

(b)

Fig.5 Voltage ratio M_v and efficiency versus different frequency at various load model

capacitors should be designed in some other ways.

In Fig.5, it shows the variation of M_v and the efficiency versus different operating frequency at various load. The compensation capacitors C_1, C_2 are determined by equations(10)(11) at 50kHz.

As can be seen from Fig.5 (a), the voltage ratio shows a growing trend as the load rises at the frequency deviating from 50 kHz. It is important that M_v is identical for the different load at 50 kHz where the system can output a constant voltage. Therefore, the compensation capacitors can be determined at an expected operating frequency based on equations (11), (12). In Fig.5 (b), we can clearly see the variation trend of the efficiency which has two peaks as the operating frequency varies. When the operating frequency is lower than 75 kHz, the efficiency corresponding to the smaller resistance is higher. However, this trend reverses with the increasing of frequency. Thus, the operating frequency shouldn't be a high value when the equivalent resistance is small.

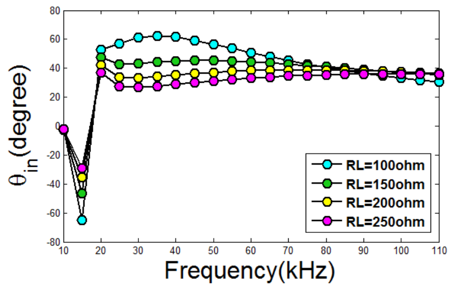

Fig.6 Input angle versus frequency at various load

For the H-bridge inverter adopted in this experiment, an inductive impedance is necessary to realize a soft switching for better efficiency. θ_{in} denotes the input angle between the input voltage and current. The value of θ_{in} is derived as

$$\theta_{in} = \frac{180^\circ}{\pi}\tan^{-1}\left[\frac{\mathrm{Im}(Z_{in})}{\mathrm{Re}(Z_{in})}\right] = \frac{180^\circ}{\pi}\tan^{-1}\left[\frac{R_L(\omega M)^2}{R_L{}^2 A(\omega) - B(\omega)Q(\omega)}\right] \quad (14)$$

Where operator Im() denotes the imaginary part of a complex number and operator Re() denotes the real part of a complex number.

In Fig.6, it shows the variation of the input angle θ_{in} versus different operating frequency at various load. The compensation capacitors C_1, C_2 are also determined at 50kHz. It can be seen that during the frequency section 10 kHz-20 kHz, the sign of the input angle has a saltation so that Z_{in} varies from capacitive state to inductive state. As a result, operating at frequency over 20 kHz can provide a soft switching. As the frequency increases, the input angle nearly keeps unchanged. Within the vicinity of 50 kHz, the lower load corresponds to the higher input angel with the higher power transferred to the load.

IV. *Experiment*

A. *Hardware design*

Table I Circuit parameters

L_1	983.3uH	L_2	611.4uH
R_1	0.72ohm	R_2	0.53 ohm
d_1	315 mm	d_2	285 mm
M	647.5uH	d	15mm
C_1	87.35nF	C_2	79.28nF

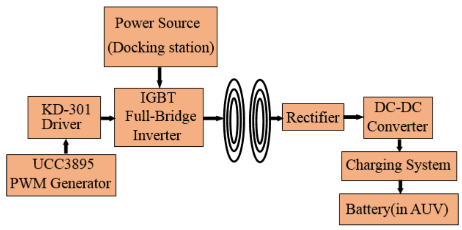

Fig.7 Schematic of IPT system

An open-loop system for the inductive contactless power transfer is shown in Fig.7. The DC voltage for IGBT full-bridge inverter is given by the docking station, which is powered by the seafloor observatory network with 375 volt. The chip UCC3895 provides 50 kHz PWM square waveform to control the switching of IGBT with the driver KD-301.By electromagnetic induction, the variable magnetic field induces alternating current in the secondary side. Using a rectifier bridge, the alternating voltage is converted to dc voltage. A DC-DC module, like Vicor-V300B48C250B, can be utilized to transform the power between IPT system and battery charging circuit. In this way, the whole system operates normally during the charging process.

The parameters of two coils are prefixed according to the geometry of the AUV and the docking station. The compensation capacitors are calculated based on equation (11), (12) at 50kHz.The details of winding parameters are listed in Table I. C_1 consists of a parallel combination of capacitors, 39nF and 47nF, and C_2 is composed of a parallel combination of capacitors, 56nF and 22nF.

B. Experimental verification

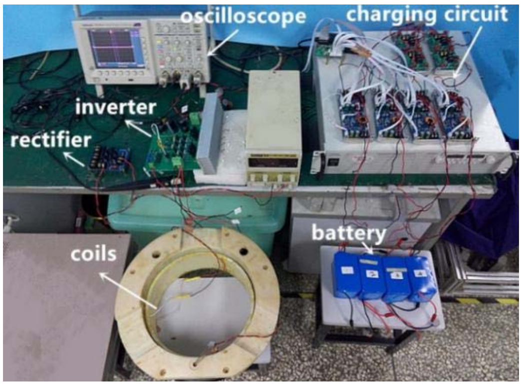

Fig.8 Implement of proposed system

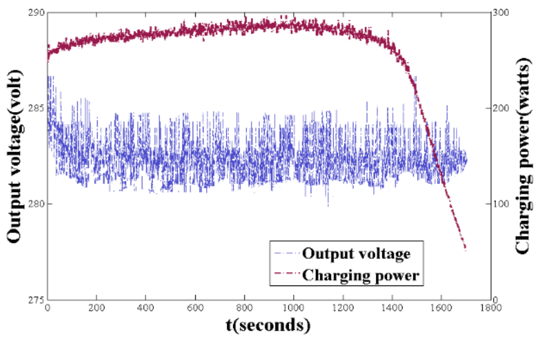

Fig.9 Sampling data about output voltage and charging power

In Fig.8, it shows the platform of the IPT system. During the charging process, the output voltage was proved to be stable as shown in Fig.9.The load voltage varied between 280 and 287 volt and nearly kept unchanged, which had good agreement with the analysis. The variation of charging power also met with the CC-CV intelligent charging process. The maximum efficiency of the system is 80%, which lies at the point of peak charging power.

V. Conclusion

Inductive power transfer is widely utilized in contactless charging system. In this paper, a novel design process applied to the underwater docking system is proposed.Serial-serial (SS) topology is selected for application for the constant output voltage. Different tests of the model are conducted to verify the theoretical analysis. The system is proved to operate with a high efficiency up to 80%.Finally the battery can be recharged reliably and stably during the CC-CV process.

Acknowledgments

Grateful acknowledgment is given to the financial supports from the National High-Tech R&D Program of China (No.2013AA09A414) and the National Natural Science Foundation of China (No.51221004).

Reference

[1]Kojiya, T.,Sato, Fumihiro. , Matsuki, Hidetoshi., 2004. Automatic power supply system to underwater vehicles utilizing non-contacting technology,In: OCEANS '04 MTS/IEEE, pp. 2341-2345.

[2]Coulson R, Lambiotte J, Pantelakis T., 2008Inductive power transfer system for underwater application.US patent 20080001696A1.

[3]Allen B, Allen B, Austin T, et al, Autonomous Docking Demonstrations with Enhanced REMUS Technology. OCEANS '06 MTS/IEEE, pp 1-6.

[4]D.Pyle, R.Granger, B.Geoghegan,2012.Leveraging a Large UUV Platform with a Docking Station to Enable Forward Basing and Persistence for Light Weight AUVs. In: OCEANS 2012 - Hampton Roads, VA, pp.1-8.

[5]H. Fukuda N. Kobayashi K. Shizuno.2013.New Concept of an Electromagnetic Usage for Contactless Communication and Power Transmission in the Ocean. In:UT Symposium'2013 IEEE-Tokyo,pp:1-4.

[6]Boys, J.T., Covic, G.A., Green, A.W. ,2000.Stability and control of inductively coupled power transfer systems. IEE Proceedings - Electric Power Applications, Vol.147,pp.37-43.